Contrib Mineral Petrol (1996) 123: 335–344

Leslie L. Baker · Malcolm J. Rutherford

Sulfur diffusion in rhyolite melts

Received: 26 April 1995 / Accepted: 1 November 1995

Abstract Diffusion rates for sulfur in rhyolite melt have been measured at temperatures of 800–1100° C, water contents of 0–7.3 wt%, and oxygen fugacities from the quartz-fayalite-magnetite buffer to air. Experiments involved dissolution of anhydrite or pyrrhotite into rhyolite melt over time scales of hours to days. Electron microprobe analysis was used to measure sulfur concentration profiles in the quenched glasses. Regression of the diffusion data in dry rhyolite melt gives $D_{sulfur}=0.05 \cdot \exp\left\{\frac{-221 \pm 80}{RT}\right\}$, which is one to two orders of magnitude slower than diffusion of other common magmatic volatiles such as H_2O, CO_2 and Cl^-. Diffusion of sulfur in melt with 7 wt% dissolved water is 1.5 to 2 orders of magnitude faster than diffusion in the anhydrous melt, depending on temperature. Sulfur is known to dissolve in silicate melts as at least two different species, S^{2-} and S^{6+}, the proportions of which vary with oxygen fugacity; despite this, oxygen fugacity does not appear to affect sulfur diffusivity except under extremely oxidizing conditions. This result suggests that diffusion of sulfur is controlled by one species over a large range in oxygen fugacity. The most likely candidate for the diffusing species is the sulfide ion, S^{2-}. Re-equilibration between S^{2-} and S^{6+} in oxidized melts must generally be slow compared to S^{2-} diffusion in order to explain the observed results. In a silicic melt undergoing degassing, sulfur will tend to be fractionated from other volatile species which diffuse more rapidly. This is consistent with analyses of tephra from the 1991 eruption of Mount Pinatubo, Philippines, and from other high-silica volcanic eruptions.

L.L. Baker (✉) · M.J. Rutherford
Department of Geological Sciences, Brown University, Providence, RI 02912, USA

Editorial responsibility: T.L. Grove

Introduction

Understanding the behavior of magmatic volatiles is increasingly important in the study of volcanic systems. In particular, familiarity with the diffusion behavior of volatile species is essential for studies of volatile transport in magmatic systems, and in estimation of the nature and extent of eruptive degassing. While recent studies have greatly increased our knowledge of diffusion rates in magma for species such as H_2O, OH^-, CO_2 and Cl^- (Watson 1982, 1991; Zhang et al. 1991), there are few data on sulfur diffusion rates, despite the fact that sulfur is an important volatile component of both mafic and silicic magmatic systems. The aim of this study was to determine the diffusion rate of sulfur in rhyolite melt, and to examine how this affects degassing of sulfur relative to other volatiles such as water and carbon dioxide. We chose experimental conditions which would make the results of the study applicable to shallow-crustal silicic magma systems.

The valence state of sulfur depends strongly on the intrinsic oxidation state of its environment. Previous studies (Nagashima and Katsura 1973; Katsura and Nagashima 1974; Carroll and Rutherford 1985, 1987, 1988) have determined how sulfur dissolves and speciates in magmas of differing oxygen fugacity and composition; Fig. 1 shows results from these studies, as well as more recent data sets on natural back-arc basalt glasses (Nilsson and Peach 1993) and mid-ocean ridge basalts (Wallace and Carmichael 1991).

In reduced magmas, defined here as those with oxygen fugacities below those defined by the Ni-NiO (NNO) buffer, sulfur dissolves primarily as sulfide ions (S^{2-}). The correlation between sulfur solubility and melt Fe content at reducing conditions suggests that sulfide associates preferentially with iron in the melt (Haughton et al. 1974; Mathez 1976). In magmas with oxidation states two or more log units above NNO, sulfur occurs dominantly in the redox state S^{6+}, and dissolves in the melt as sulfate ions, SO_4^{2-} (Katsura and Nagashima 1974; Car-

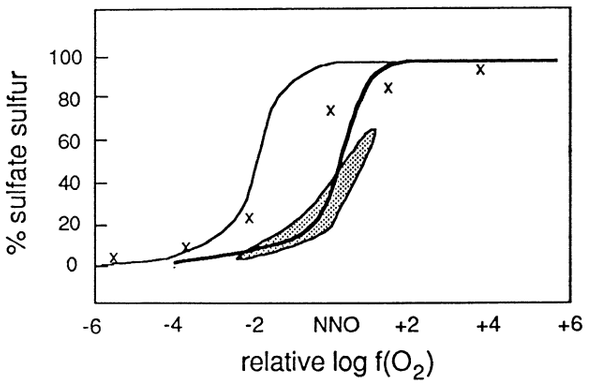

Fig. 1 Sulfur speciation in silicate melts vs log oxygen fugacity relative to the nickel-nickel oxide (NNO) buffer. *Heavy curve* is from experimental data of Carroll and Rutherford (1988) on andesite and dacite melts. *Light curve* is from experimental data of Nagashima and Katsura (1973) on Na_2O-3SiO_2 melts; the relatively high sulfate contents of these melts are probably due to their high alkali contents. *Crosses* show data from Katsura and Nagashima (1974) on tholeiite basalt melt. *Stippled field* shows location of natural back-arc basalt glasses (Nilsson and Peach 1993) and mid-ocean ridge basalt glasses (Wallace and Carmichael 1991)

roll and Rutherford 1988). In magmas of intermediate oxygen fugacity (NNO to NNO + 2), sulfur is thought to exist in the melt as a mixture of these two species. In alkali-rich magmas, however, sulfate is stabilized to lower oxygen fugacities, as shown in Fig. 1 (Nagashima and Katsura 1973). It is possible to determine the speciation of sulfur in a glass either by using the electron microprobe to measure the wavelength shift of sulfur X-rays which occurs with the change in speciation (Carroll and Rutherford 1988), or by wet chemical analysis (Nagashima and Katsura 1973; Katsura and Nagashima 1974). Recent analyses of naturally occurring glasses (Wallace and Carmichael 1992; Nilsson and Peach 1993) confirm the gradual shift in speciation with changing oxidation state observed in the experimental samples (Fig. 1).

Previous and ongoing studies (Watson et al. 1993; Watson 1994) have examined the diffusion of sulfur (present as S^{2-}) in melts at reducing conditions and 10 kbar pressure. The results of this earlier work show that diffusion of sulfur in reduced melts is slower by several orders of magnitude than diffusion of other volatile species such as H_2O and CO_2. The results also show that increasing melt water content may increase diffusivity of sulfur by several orders of magnitude, as it does the diffusion rate of many other melt species.

A few data for the rate of sulfur transport in SiO_2-CaO-Na_2O melts equilibrated under air were given by Brückner (1961, 1962). The diffusivities calculated by Brückner are very high, on the order of 10^{-5} to 10^{-6} at 1300° C. These experiments have clearly been affected by convection, and Brückner (1962) admitted that they are at best an upper limit. These transport rates are far faster than those given by Watson (1994) for anhydrous melts, and it is likely that they are not representative of diffusive transport of sulfur, but rather of convection.

The difference in dissolved sulfur species with varying oxygen fugacity suggests the possibility of a corresponding difference in diffusion rate. Under reducing conditions, diffusion of sulfur and oxygen may be broadly similar, because O^{2-} and S^{2-} have the same charge and are of comparable size: 1.26 and 1.70 Å, respectively (Shannon 1976). In oxidized melts, sulfur might diffuse either as the SO_4^{2-} complex or as S^{6+}; the large size of the former and the high charge of the latter would tend to inhibit diffusive motion. In melts which contained a mixture of sulfur species, the faster-diffusing species (probably S^{2-}) would likely dominate transport.

We have conducted experiments to measure the diffusion of sulfur at conditions typical of shallow (1–10 km), oxidized magmatic systems. Under these conditions, most or all of the sulfur dissolved in the melt is in the oxidized form (SO_4^{2-}; Carroll and Rutherford 1988). We have also conducted a few experiments at similar temperatures and pressures but more reducing conditions, and several experiments under extremely oxidizing conditions, to determine the effect of changing oxygen fugacity on the rate of sulfur diffusion.

Experimental and analytical methods

The experiments in this study were performed using a natural metaluminous rhyolite (Table 1). Samples of this rhyolite glass were ground under ethanol in an agate mortar and pre-equilibrated at the experimental pressure, temperature and oxygen fugacity with water slightly in excess of that required to saturate the melt at the experimental pressure. The resulting water-saturated glasses were reground to a powder under ethanol in an agate mortar. Natural crystalline anhydrite was used as a source of sulfur in oxidized experiments; hand-picking ensured that only clear, euhedral grains were used for this purpose. Natural pyrrhotite was used as a sulfur source in reduced experiments in which anhydrite was not stable; pyrrhotite grains were hand-picked to avoid contamination by accessory phases. The pyrrhotite and anhydrite compositions were verified by energy dispersive spectrometry (EDS): the pyrrhotite contained only Fe and S, and the anhydrite contained only Ca, S and O, to the 0.1% certainty level.

Figure 2a shows the configuration of a typical oxidized experiment. A single grain of anhydrite was placed between layers of the

Table 1 Starting composition, Los Possos obsidian

Oxide	Wt%
SiO_2	76.6
Al_2O_3	12.3
FeO*	1.05
MgO	0.04
TiO_2	0.08
Na_2O	4.41
CaO	0.37
K_2O	4.64
MnO	0.05
Total	99.56
FeO [a]	0.74
Fe_2O_3 [b]	0.34

[a] FeO measured by titration
[b] $Fe_2O_3 = 1.1113 \cdot (FeO^*\text{-}FeO)$

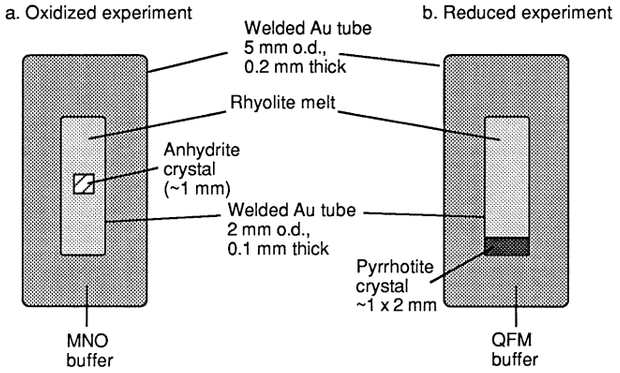

Fig. 2a Configuration of anhydrite dissolution experiment. Experiments were run horizontally in cold-seal vessels, except at 1000° C where they were run vertically in TZM vessels. MNO buffer = MnO + Mn_3O_4 ± H_2O. **b** Configuration of pyrrhotite dissolution experiment. Experiments were run vertically as shown, in TZM vessels. QFM buffer = quartz + fayalite + magnetite ± H_2O

powdered, water-saturated glass inside a gold tube which was then sealed. No additional water was added to this tube. The viscosity of the rhyolite melt was high enough to prevent the anhydrite crystal from sinking through the melt beneath it. For runs buffered with the solid assemblage MnO-Mn_3O_4 (MNO), the small, sealed charge was placed inside a larger, sealed gold tube which contained water and the solid buffer materials. One experiment (#87) was run at the intrinsic oxygen fugacity of the Rene metal pressure vessel and its nickel filler rod, which is approximately one log unit above the nickel-nickel oxide (NNO) buffer (Rutherford and Hill 1993); in this case the small, sealed tube was placed directly into the pressure vessel. Oxidized experiments at ≥900° C were run in horizontal furnaces in Rene metal cold-seal vessels pressurized with water; those at 1000° C were run vertically in TZM vessels pressurized with argon. Reduced experiments (Fig. 2b) were buffered with the assemblage quartz-fayalite-magnetite (QFM). All reduced experiments were run vertically in TZM vessels under argon pressure. Experimental configurations were otherwise as described above, except that the pyrrhotite grain was placed in the bottom end of the small gold tube to prevent it from sinking through the melt.

Experimental conditions are summarized in Table 2; they range from 800 to 1100° C, from 1 atm (0.101 MPa) to 2 kbar, and from moderately reducing conditions (QFM buffer) to very oxidized (run in air). Experiments in Rene bombs were quenched in a jet of high-pressure air. Experiments in TZM were quenched by plunging the pressure vessel and sheath into cold water.

Several experiments (# 97, 101, 125) were run under anhydrous conditions. The small sample tubes in these experiments were left unsealed and were placed in large tubes containing anhydrous buffer materials. This allowed direct exchange of vapor between the buffer materials and the sample. Thus these samples were not oxygen buffered as effectively as the hydrous experiments. Because the experimental starting glass had been pre-equilibrated at the experimental oxygen fugacity, the dry buffer was needed only to prevent changes in the pre-set oxygen fugacity of the experimental sample. The speciation of sulfur in the glasses from these experiments indicated that they did not undergo large changes in oxygen fugacity.

Two experiments with water contents of 2–3 wt% (#92 and 100) were not H_2O saturated at run pressures, which means their oxygen fugacities were not buffered because buffering requires the presence of a hydrogen–bearing fluid when used in sealed tubes. As with the anhydrous experiments described above, these samples were pre-annealed at the experimental oxygen fugacity and were run in sealed tubes surrounded by the oxygen buffer assemblage, presumably preventing significant change in the intrinsic oxygen fugacity of the sample.

A few experiments (# 108, 111 and 113) were performed at 1 atm (0.101 MPa) and 1000–1100° C in air, in order to examine sulfur diffusion under anhydrous and very oxidizing conditions. The starting glass powders for these experiments were first fused in air at 1000–1100° C for several days; a few microscopic crystals of hematite occurred in these glasses, indicating that it achieved a very high oxidation state, but the glass FeO content as measured by electron microprobe was not measurably lower than those in the starting material (Table 1). From this glass starting material, charges were prepared as described above, suspended in a furnace for several days and then drop-quenched in water. Experiments at temperatures below 1050° C were run in Au tubes, while those at higher temperatures were run in Pt tubes. At temperatures of 1000° C and above, anhydrite is unstable in air; it was therefore necessary that the crystal be completely surrounded with melt during the entire duration of the experiment to protect it from breakdown.

Polished thin sections of the resulting glasses were prepared (under ethanol when necessary, to avoid conversion of anhydrite to gypsum) and analyzed on a Cameca Camebax electron microprobe. Each sample was analyzed twice: once for sulfur content, and once for major element composition and estimation of volatiles by difference (Devine et al. 1995). Sulfur analyses were obtained along transects perpendicular to the anhydrite or pyrrhotite crystal edge, beginning at 10–50 μm from the crystal surface. This helped to ensure that the first analysis was of sulfur-saturated glass but was not contaminated by secondary X-ray fluorescence from the crystal itself. Secondary X-ray contamination was occasionally a problem, and abnormally high estimates of S content were removed from the dataset before the data were regressed. In anhydrite-bearing charges, the crystal was sometimes removed from the thin section by a combination of picking and ultrasonic cleaning, in order to obtain good analyses of the glass S content very near the crystal-glass contact. For S analyses, we used a 1–5 μm beam, an accelerating voltage of 15 kV and a beam current of 30 nA. Standard ZAF corrections were applied. In oxidized experiments, sulfur was analyzed at the sulfate peak position, whereas in reduced experiments, it was analyzed at the sulfide peak position. For major element analyses, we used an accelerating voltage of 15 kV, a beam current of 10 nA, and 5–10 μm beam. Sodium loss from the glass was corrected for in major element analyses using the method of Nielsen and Sigurdsson (1981). Some experimental glasses contained bubbles from slight oversaturation with H_2O; these bubbles were easily avoided, and S analyses were conducted far away from them in order to ensure that the bubbles did not affect the measured diffusion profiles.

The low solubility of sulfur in the melt was the cause of most of the analytical difficulties in this study. At lower temperatures (800° C), sulfur solubility in silicic melts is on the order of 80 ppm (Carroll and Rutherford 1987). As the microprobe detection limit for sulfur is roughly 30 ppm, this leaves a very small window for detection of sulfur. We compensated for this by using a high beam current (30 nA) and long counting times (100 s). At higher temperatures, the sulfur solubility rises quickly and detection limits become less of a problem. In long experiments at higher temperatures and oxidizing conditions, the anhydrite crystal began to decrepitate around the edges; this complicated the geometry of the experiment because the crystal-melt boundary was no longer fixed. This problem was eliminated by limiting the duration of hydrous high-temperature experiments. Runs of several hours in length produced reasonable diffusion profiles (Fig. 3) but left the crystals intact and their edges sharp, and ensured that the crystal-melt interface was stationary for the duration of the experiment. Experiments showing significant decrepitation of the anhydrite and movement of the crystal-melt boundary have not been included in this study. Decrepitation of pyrrhotite was not observed in experiments carried out under reducing conditions.

The use of a high beam current and long count times to compensate for low sulfur solubility limited the number of data points

Table 2 Summary of run information, water contents and diffusivity data

Expt	Buffer [a]	T [b] (°C)	H_2O (wt%)	P (bars)	Duration (s)	log D: avg (cm^2/s)	log D: transect (cm^2/s)	R [c]
93	MNO	800	5.6	2000	70200	−10.09	−10.09	0.87
82	MNO	850	3.2	125	10800	−10.22	−10.38	1.00
							−10.06	0.95
74	MNO	850	6.7	2000	17100	− 9.28	− 8.91	0.86
							− 9.41	0.94
							− 9.53	0.90
85	MNO	900	2.8	125	75600	−10.93	−10.93	0.76
79	MNO	900	4.7	800	14700	− 9.70	−10.14	0.98
							− 9.48	0.93
							− 9.48	0.91
95	MNO	900	6.1	2000	21600	−10.05	−10.24	0.98
							− 9.84	0.90
							−10.08	0.95
91	MNO	900	6.2	2000	9000	− 9.55	− 9.61	0.88
							− 9.52	0.93
							− 9.52	0.85
75	MNO	900	7.1	2000	16200	− 8.94	− 8.96	0.95
							− 8.91	0.97
97	MNO	1000	0.0	2000	263400	−10.51	−10.52	0.71
							−10.43	0.87
							−10.58	0.82
92	MNO	1000	2.6 [d]	800	18000	− 9.67	− 9.50	0.78
							− 9.60	0.79
							− 9.90	0.66
84	MNO	1000	7.2	2000	18000	− 9.04	− 8.60	0.91
							− 9.16	0.96
							− 9.35	0.94
125	MNO	1100	0.0	1000	68400	−10.78	− 9.95	0.93
							−11.61	0.80
87	NNO+1	900	7.3	2000	14400	− 9.58	− 9.48	0.96
							− 9.55	0.96
							− 9.69	0.90
101	QFM	1000	0.0	1000	80100	− 9.75	− 9.54	0.79
							− 9.97	1.00
100	QFM	1000	2.3 [d]	2000	21600	− 9.04	− 9.15	0.78
							− 9.29	0.98
							− 8.68	0.97
108	AIR	1015	0.0	1	167400	−11.43	−11.91	0.89
							−10.92	0.54
							−10.92	0.96
							−11.92	0.97
							−11.34	0.88
							−11.60	0.80
111	AIR	1050	0.0	1	154800	−12.04	−11.74	0.83
							−12.33	0.89
113	AIR	1100	0.0	1	180000	−11.44	−11.37	0.97
							−11.52	0.99

[a] Experiments at QFM used pyrrhotite as sulfur source; all other experiments used anhydrite
[b] Experiments at ≥1000°C were run vertically in TZM vessels using argon as pressure medium. All other experiments were run horizontally in cold-seal vessels using water as pressure medium
[c] R from error function fits of individual profiles
[d] Denotes water-undersaturated experiments

which could be collected along each profile. Even at lower currents than 30 nA, an electron beam will rapidly damage the surface of a hydrous rhyolite glass, causing loss of volatile components such as sodium and sulfur. At each analysis point in the water-saturated glasses in this study, the focused beam produced damage spots of 5–10 μm across. Avoiding previously damaged glass when conducting the analyses resulted in the points being 5–10 μm apart. Thus, taking steps to lower the counting error in sulfur-poor glasses caused an unavoidable increase in the uncertainty of the profile shapes.

To calculate diffusion rates, we used the solution to Fick's second law for a semi-infinite source, which we conclude is appropriate for our experimental setup over the relatively short time scales used in this study. The solution we used is:

$$\frac{C_x - C_0}{C_i - C_0} = \mathrm{erf}\left\{\frac{x}{2\sqrt{D_i t}}\right\} \quad (1)$$

where C_0 is the (constant) sulfur concentration at the interface, C_i is the initial sulfur content of the melt, and C_x is the concentration at distance x from the interface (Crank 1975). Iteratively solving for the inverse error function of the concentration ratio, and regressing it against the distance x from the interface, allowed us to calculate the diffusion rate from this expression.

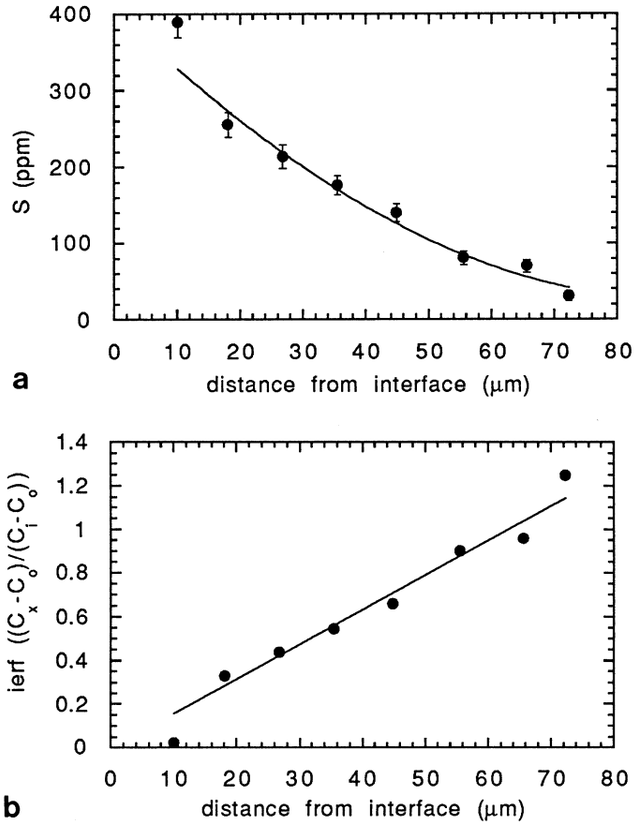

Fig. 3a A typical diffusion profile from anhydrite dissolution experiment (# 75, profile 1) at 900°C, 2 kbar, MnO-Mn_3O_4 buffer. Error bars show one standard deviation. *Solid curve* shows profile calculated from error function fit to data. Point at 10 μm distance may have been affected somewhat by secondary X-ray fluorescence; however, removing it from dataset has virtually no effect on error function fit, so it has been retained. **b** Inverse error function of concentration ratio for data in Fig. 3a. *Solid line* shows error function fit to data

To use this solution to the diffusion equation, it is necessary that C_0, the sulfur concentration at the interface, be equal to the sulfur solubility limit at the experimental conditions. Preliminary experiments determined that the sulfur solubility limits in the rhyolite glass range linearly from 250 ppm at 800° C to 700 ppm at 1000° C. Analyses of dissolved S concentrations at the glass-crystal contact in charges where the anhydrite crystal had been removed (to prevent secondary X-ray contamination from the anhydrite crystal, as described above) showed that the melts achieved S saturation at the interface during the experiments.

Figure 3a shows a typical profile from an experiment (LP 75) run at 900° C and 2 kbar; Fig. 3b shows the error function fit to the same profile. The high S content of the point at 10 μm distance in this profile may be due to secondary X-ray fluorescence from the anhydrite crystal. Nonetheless, regressions of the data with and without this point are virtually identical; the calculated curve shown includes this data point. Because diffusion in our experiments was taking place away from the anhydrite crystal on all sides, we analyzed along transects away from every face of the anhydrite crystal which had a good crystal-glass interface. We used these multiple analyses to calculate error bars for the results. Agreement among different transects in the same experiment was good. Transects away from different crystal faces in the same experiment showed no systematic differences. Table 2 lists individual

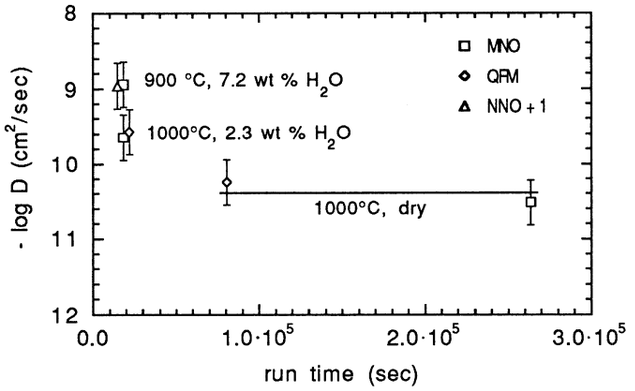

Fig. 4 Measured diffusion coefficients plotted against run time for pairs of experiments at identical temperature and water content. *Error bars* show one standard deviation, based on the variation between different transects measured on the same experiments (Table 2). *Horizontal line* for anhydrous experiments at 1000° C is at average log D for this experiment pair

transects and their calculated D values and error estimates, as well as average D values for each experiment. Because of errors in our original error function calculation, the diffusivities given here are lower than those initially published (Baker and Rutherford 1994) by one-half to one order of magnitude.

Results

Diffusion control of experimental kinetics

Several observations suggest that diffusion of sulfur, rather than crystal-surface processes, was the rate-controlling factor in our experiments. We conducted pairs of experiments at identical temperatures and water contents but different run times, and in some cases using different sulfur sources. Were surface processes a rate-controlling factor, experiments with run times that differed by more than a factor of two would yield different apparent diffusion rates. Figure 4 shows several such experiment pairs, all of which yield estimated diffusion rates that agree within experimental error. Furthermore, if surface processes were controlling diffusion kinetics, then experiment pairs run at identical temperature and water content but with different sulfur sources (anhydrite vs. pyrrhotite) should yield significantly different estimates of diffusion rate. Figure 4 shows that the estimates of diffusion rate from such experiment pairs (at 900° C, 7.2 wt% H_2O, and 1000° C, anhydrous) agree well.

Diffusion of sulfur within the source crystal should likewise not be affecting the measurements made in this study. The total amount of sulfur which must be extracted from the crystal to produce profiles such as those observed in this study is very small, because the profiles generated in the experiments were very short, and because sulfur saturation levels were a few hundred ppm at most. This indicates that sulfur diffusion within the anhydrite crystal was not a rate-controlling process during the experiments.

Sulfur saturation was achieved at the anhydrite-melt boundary in all experiments, although sulfur saturation levels were slightly different from those found in other studies (Carroll and Rutherford 1988; Luhr 1990). The experiments in this study indicated sulfur saturation levels which increased linearly from approximately 250 ppm at 800° C to approximately 700 ppm at 1000° C. These sulfur contents are lower at high temperatures than those found by Carroll and Rutherford (1988) and Luhr (1990); this may be due to the higher Fe contents of the magmas used in those studies.

Diffusion rates and activation energies

Results from all our experiments except those run in air show that there is no change in the rate of sulfur diffusion between oxidized and reduced melts (Fig. 5). As discussed above, the primary dissolved sulfur species changes from S^{2-} in the reduced melt to SO_4^{2-} in the oxidized melt. If these were also the diffusing species, then the diffusion rate of sulfur might be expected to change with oxygen fugacity because of the difference in size between these two ions. The observation that it does not change suggests that one species controls sulfur diffusion over the range of conditions studied in the experiments. This result is better illustrated in Fig. 4, where diffusion rates are plotted for pairs of experiments run at the same temperature and water content but different oxygen fugacities. These diffusion data agree extremely well despite the large difference in oxygen fugacity between the members of each pair. As a result, we believe the data in Fig. 5 to represent the diffusion of a single species.

The range of experimental *P-T* conditions over which we examine sulfur diffusion may be extended by including the data of Watson (1994) from experiments done in a piston cylinder apparatus at 10 kbar, 1100–1500° C and 0–8.5 wt% water (Fig. 6). While these experiments were not oxygen buffered, the use of Mo capsules and graphite furnaces ensured that they ran at very reduced conditions. Figure 6 shows that the sulfur diffusion rates measured in rhyolites in their experiments are consistent with those reported in this study, despite the differences in oxygen fugacity, temperature, pressure and experimental method between the two investigations.

Although the results will be subject to large uncertainties, it is possible to estimate from our results the activation energy for sulfur diffusion in a dry melt. Regressing the three data points at zero water content in Fig. 5 gives:

$$D_S = 0.05 \cdot \exp\left\{\frac{-221 \pm 80}{RT}\right\} \quad (2)$$

where D is in cm^2/sec and Q is in kJ/mol. If the data used in the regression also include the single point at zero water given by Watson (1994), the expression becomes:

$$D_S = 0.01 \cdot \exp\left\{\frac{-205 \pm 24}{RT}\right\} \quad (3)$$

The error in this expression is significantly smaller because the Watson datum was measured at a much higher temperature than those in this study, but the value for the activation energy is not significantly changed, giving additional confidence to the grouping of the two datasets.

Also in Fig. 6, the results of our experiments run in air are compared with summarized data from less oxidizing conditions. There is approximately an order of magnitude difference in the diffusion rates between experiments in air and those buffered at MNO or lower oxygen fugacities. One possible explanation for this slowdown in sulfur transport is that S^{2-} is no longer abundant enough

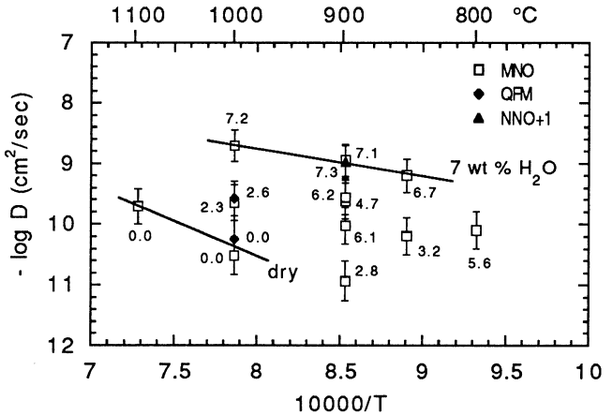

Fig. 5 Arrhenius diagram showing diffusivity of sulfur. Dissolved water contents are indicated by the *small numbers* next to the data points. The line marked *dry* is a best-fit line to the three data points with 0 wt% water. The line marked *7 wt% water* is a best-fit line to the four points with 7 ± 0.3 wt% water. Error bars as in Fig. 4

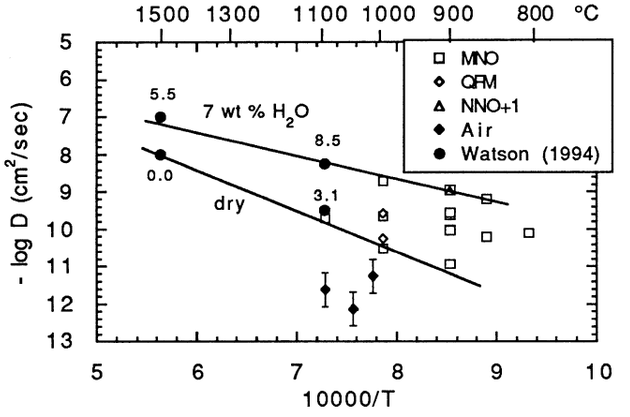

Fig. 6 Data from this study compared with data from Watson (1994), for sulfur diffusion measured in rhyolites. Nominal water contents for experiments by Watson (1994) are indicated by the numbers next to the data points. Best-fit lines from Fig. 5 are shown extrapolated to 1500°C. The three points at very low diffusivity are from experiments which were run in air

in the melt to control sulfur diffusion, so a different (and slower-diffusing) species has taken over control of diffusion in these extremely oxidized melts.

Discussion

Diffusing species

It seems likely that, over almost all the conditions examined both in this study and others (Watson et al. 1993; Watson 1994), a single species is dominating the diffusion of sulfur. This is analogous to diffusion of water (Zhang et al. 1991), which dissolves into melts as a mixture of hydroxyl ion (OH^-) and molecular H_2O in varying amounts depending on pressure and temperature. Even when the dominant dissolved chemical species is hydroxyl ion, diffusion is in almost all cases controlled by molecular water rather than by hydroxyl ion. This occurs because D_{H_2O} is much larger than D_{OH^-}, so that transport of molecular water far outpaces that of hydroxyl. The primary difference between water and sulfur is that water speciation is dependent on total water content (Stolper 1982), whereas sulfur speciation appears to be independent of total melt sulfur content at otherwise constant conditions (Carroll and Rutherford 1988; Nilsson and Peach 1993).

The sulfur species which are most likely to control diffusive transport in the melt are S^{2-} and S^{6+} (or SO_4^{2-}). Either or both of these species have been detected in silicate melts over a wide range in composition and oxygen fugacity, as discussed in the introduction. While it is possible that some other sulfur species such as S_2 or S^{4+} is controlling diffusion behavior, we consider this to be unlikely, because no spectroscopic evidence has been reported which suggests that such dissolved species exist in measurable quantity in the melt. We suggest that the primary diffusing sulfur species is the sulfide ion. The fundamentals of ionic diffusion suggest that sulfide should diffuse much faster than either S^{6+}, which is highly charged, or SO_4^{2-}, which is a large ionic complex. Moreover, the fact that sulfur diffusion is slowest in the most oxidized dry melts (Fig. 6) suggests that a more reduced species (i.e. S^{2-}) is controlling diffusion whenever it is present in the melt.

The activation energy for sulfur diffusion is somewhat higher than those of other volatile species (Table 3). For comparison, Table 3 shows activation energies for O^{2-}, measured in andesite (Wendlandt 1991), and a median activation energy for O^{2-} from measurements on a variety of high-silica synthetic (non-geologic) melts (Schreiber et al. 1986 and references therein). Because S^{2-} and O^{2-} have similar size and identical charge, their activation energies for diffusion in the melt should be similar. The fact that the values for the two in dry, silica-rich melts are comparable suggests that S^{2-} is the diffusing sulfur species.

Jambon (1982) showed that it is possible to estimate the activation energy for diffusion of cations based upon their charge and size, using an elastic model for diffusion through silicate melts. The model predicts that activation energy is described by the equation:

$$Q = 128\,(r-1.34)^2 + 33\,Z^2/(r+1.34) + 8 \text{ kcal/mol} \quad (4)$$

where Q is activation energy, and r and Z are the radius and charge, respectively, of the diffusing species. This model worked well for a number of cations whose diffusivities in rhyolite were measured by Jambon (1982). In addition, Carroll (1991) and Zhang et al. (1991) obtained good results from applying elastic diffusion models to diffusion of noble gases and H_2O, respectively. We have used the model of Jambon (1982) to predict activation energies for several possible sulfur species. Table 4 shows the results of these calculations, which assume octahedral coordination for all ions (though the calculation is not strongly sensitive to assumed coordination in this case). The calculated activation energy for S^{2-} is within the fairly large error of our measured value. In contrast, the activation energies for the highly-charged

Table 3 Measured activation energies for sulfur and oxygen, compared with CO_2 and H_2O

Species	Melt composition	Q (kJ/mol)	Source
S^{2-}	Rhyolite, dry	221 ± 80	Data from this study only
S^{2-}	Rhyolite, dry	205 ± 24	Data from this study and Watson (1994)
O^{2-}	Andesite, dry	251	Wendlandt (1980)
O^{2-}	High-silica melts, dry	224 ± 40	Schreiber et al. (1986) and refs therein: average and range for high-silica melts
H_2O	Rhyolite, dry	103 ± 5	Zhang et al. (1991)
CO_2	Rhyolite, dry	171 ± 74	calculated from data in Watson (1991)

Table 4 Activation energies for different sulfur species and for oxygen, calculated by the method of Jambon (1982). Measured values from Table 3 for comparison

Ion	Z	r (ionic)[a] Å	Q (calc) kJ/mol	Q (meas) kJ/mol
S^{2-}	−2	1.70	285	221 ± 80
S	0	1.04	82	
S^{4+}	+4	0.51	1597	
S^{6+}	+6	0.43	3285	
SO_4^{2-}	−2	2.5 [b]	898	
O^{2-}	−2	1.26	249	224 ± 40

[a] From Shannon (1976), except where noted, for ions in octahedral coordination
[b] Estimated from radii of component ions

sulfur cations are extremely high, implying that these species are essentially immobile in the melt. While Jambon (1982) only tested this model on cations, the theoretical basis of the model does not a priori exclude its applicability to anion diffusion. The similarity of the calculated and measured values suggests that the elastic model is a good predictor of diffusivity of sulfur anions. In addition, the elastic model predicts the activation energy for oxygen anions fairly well.

The suggestion that sulfur transport in oxidized melts is controlled by S^{2-} has implications for the kinetics of the reaction between S^{2-} and SO_4^{2-}. The diffusion of S^{2-} through an oxidized melt will result in a transient state in which melt along the diffusion profile will have a higher than equilibrium ratio of S^{2-} to SO_4^{2-}. If this ratio were to re-equilibrate locally more quickly than diffusion takes place, then diffusion of sulfur would apparently be slower under oxidizing conditions than under reducing conditions. Because sulfur which converted to sulfate would be effectively immobilized in the melt, this is analogous to the problem described by Crank (1975) of adsorption of a diffusing species. Because the sulfide to sulfate ratio appears to be constant in a melt at given conditions (i.e. not related to total sulfur concentration), we may use the simple solution for the case where the concentration of diffusing substance is proportional to the concentration of immobilized substance. If re-equilibration is effectively instantaneous with respect to diffusion, then the effective diffusion rate measured is linearly related to the true diffusion rate:

$$\frac{\partial C}{\partial t} = \frac{D}{R+1}\frac{\partial^2 C}{\partial x^2} \qquad (5)$$

where R is the ratio of immobilized substance to diffusing substance, C is concentration of the diffusing substance, t is time and x is distance from the interface (Crank 1975). This is the usual form of equation for diffusion in a semi-infinite medium, but with the diffusion coefficient given by $\frac{D}{R+1}$. In this case our experiments on reduced and oxidized melts would give different results, yielding diffusion rates which were proportional to the equilibrium ratio of sulfide to sulfate in the melt. Figures 4 and 5 demonstrate that this is not the case. Our results therefore suggest that the ratio of S^{2-} to SO_4^{2-} must re-equilibrate at a much slower rate than that at which sulfur diffuses through the melt.

In the highly oxidized experiments run in air, the apparent diffusion rate of sulfur drops by one to two orders of magnitude (Fig. 6). Because of these extremely slow diffusion rates, it is difficult to extract much reliable quantitative information from the experiments. There are two possible explanations for the apparent drop in sulfur diffusion rate in these experiments. One is that in a melt equilibrated in air, there may be virtually no sulfur dissolved as sulfide. In this case, some slower-diffusing species would take over control of diffusive transport. The diffusing species under these conditions may be S^{6+}, but this possibility seems unlikely because of the very high charge of this cation. Another possible explanation is that, under such oxidizing conditions, the rate of conversion of S^{2-} to SO_4^{2-} in the melt is greater than the rate of diffusional transport. In this case, Eq. 5 would become appropriate and the diffusion rate measured would only be an apparent one. The one to two orders of magnitude of difference between D_{sulfur} in air and D_{sulfur} at lower oxygen fugacity suggests that R is on the order of 10 to 100, or conversely that the sulfide content is between 1 and 10 percent of the total sulfur content of the melt in the samples equilibrated in air.

Degassing and fractionation

Diffusion data for several common volatile species are summarized in Fig. 7. While the diffusion rates of common magmatic volatiles tend to be broadly similar, sulfur does not follow this pattern, diffusing much more slowly than other gases such as H_2O, CO_2 and Cl. Sulfur is similar to the other important volatiles, however, in that its diffusion rate depends strongly on melt water content. The dependence of diffusivity, as well as activation energy, on melt water content may be due to the drop in melt viscosity with increasing water content (Baker 1991). It is possible that the effect of water on the rate and activation energy of sulfur diffusion is due to some interaction between dissolved S and H_2O. But because water's effect on sulfur diffusivity is similar to its effect on the diffusivity of other volatiles such as CO_2 (Watson 1991, 1994), the data do not require such an interaction to explain why sulfur transport occurs more rapidly in hydrous melts.

The data in Fig. 7 have important implications for volatile degassing from high-silica magmas. The difference in transport rate between sulfur and other volatiles will affect the rate at which a volatile-bearing melt reaches equilibrium with its surroundings. In a magma which contains a vapor phase, the gas bubbles will tend

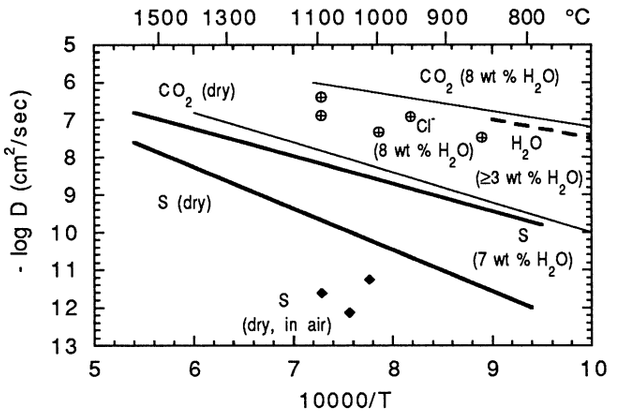

Fig. 7 Summary of diffusivities of common volatile species in rhyolite melt, after Watson (1991), and summarized data from Fig. 6

to reach their equilibrium H_2O and CO_2 contents long before they achieve their equilibrium sulfur contents. In a rapidly erupting and degassing rhyolite magma, this difference will tend to fractionate sulfur from other exsolving volatiles. Species such as H_2O and CO_2 will tend to escape from the magma at fairly similar rates and, according to available data, will partition strongly into the vapor phase. While available data on sulfur solubility suggest that sulfur will also tend to partition into the vapor phase as pressure drops (Carroll and Rutherford 1985; Luhr 1990), the slow rate of sulfur diffusion will place a practical limit on how much can be transported to the growing vapor bubbles in an erupting magma.

This is illustrated by the 1991 eruption products of Mt. Pinatubo, Philippines. Analyses of melt inclusions of the pre-eruptive Pinatubo dacite (Rutherford and Devine 1995) showed that melt inclusions trapped in plagioclase phenocrysts contained an average of 6.5 wt% H_2O, 55 $\pm$ 23 ppm S, and CO_2 below detection (50 ppm). The matrix glass of the erupted dacite contains 0.4 wt% H_2O and 36 $\pm$ 28 ppm S; CO_2 contents in the matrix glass have not been determined but are probably small (Rutherford and Devine 1995). Thus, virtually all the H_2O escaped during the eruption, but only a small fraction of the dissolved S diffused rapidly enough to reach and exsolve into vapor bubbles before the pumice was quenched.

The same pattern appears in analyses of high-silica magmas from Toba, El Chichon, Mount St. Helens, the Roseau Tuff, Hekla and Krakatau (Devine et al. 1984; Devine, personal communication 1995): while nearly all the water dissolved at depth was lost from each melt upon eruption, only a small fraction of the dissolved sulfur escaped the melt before the pumices quenched. In addition, Devine et al. (1984) found that the total amount of sulfur lost upon eruption decreases with silica content, despite the fact that the total volatile loss during eruption increases with melt silica content. Even accounting for the higher overall sulfur content of melts with lower total silica content, this still implies that the rate of diffusive loss of sulfur from the melt drops with increasing silica content. This is consistent with the data of Watson (1994), which suggest faster sulfur diffusion in andesitic and basaltic melts than in rhyolites at a given temperature. The higher temperatures at which low-silica melts are erupted will also encourage more complete degassing of sulfur from mafic melts than from silicic ones.

The observation that sulfur degassing from high-silica melts should be inefficient exacerbates the problem of "excess" sulfur degassing during some volcanic eruptions. Many explosive volcanic eruptions have been observed to produce more sulfur vapor than could possibly have been dissolved in the erupted magma at magma chamber conditions (Luhr et al. 1984; Westrich and Gerlach 1992; Gerlach and McGee 1994). The diffusion data presented in this study suggest that sulfur dissolved in the melt is likely to provide an even smaller fraction of the sulfur degassed in these eruptions than was previously thought, unless degassing takes place over a much longer time scale than that of the eruption itself. These results suggest that the "excess" sulfur source must be one which is not subject to the kinetic control of sulfur diffusion through the melt.

Conclusions

We have determined diffusion rates for sulfur in rhyolitic melt over a range of oxygen fugacity, temperature and water content. These data suggest that changing oxygen fugacity does not in most cases affect the rate of sulfur diffusion, despite evidence that it strongly affects sulfur speciation. This suggests that a single sulfur species is controlling the diffusion of sulfur over most of the range of conditions studied.

Several lines of evidence suggest that the diffusing species over a wide range of melt oxidation states is sulfide ion (S^{2-}), even where this is not the dominant sulfur species dissolved in the melt. A corollary of this hypothesis is that local oxidation-reduction reactions between S^{2-} and SO_4^{2-} occur slowly relative to S^{2-} diffusion in both wet and dry melts. At the very high oxidation states reached by experiments in air, the rate of sulfur diffusion drops by one to two orders of magnitude relative to less oxidized experiments. It is possible that these extremely oxidized melts no longer contain significant S^{2-}, and that sulfur diffusion in them is controlled by some other species. Alternatively, it may be that the rate of conversion from S^{2-} to SO_4^{2-} has increased in these melts to the point where it outpaces diffusive transport of S^{2-}, causing an apparent slowdown in sulfur diffusion.

These very slow diffusion rates will tend to result in fractionation of sulfur from other magmatic volatiles during eruption and degassing of high-silica melts. During rapid degassing such as takes place in explosive eruptions, most of the sulfur dissolved in a melt will be unable to escape from the glass before quenching. This is in contrast to other volatiles such as H_2O and CO_2, which are degassed much more efficiently.

Acknowledgements The authors owe thanks to Bruno Giletti, John Farver, Harold Smith, Jim Greenwood, and particularly to Dan Brabander for many helpful discussions, and for their thoughtful comments on an earlier version of this manuscript. Joe Devine kindly provided access to unpublished data, as well as helpful comments on the manuscript and able assistance with the microprobe analyses. Two anonymous reviewers also provided comments which improved the manuscript. This work was funded by NSF grant # EAR 92–18816, and by a NASA Graduate Research Fellowship to the first author.

References

Baker L, Rutherford MJ (1994) Diffusion rates of sulfur (S^{6+}) in hydrous silicic melts. EOS Trans Am Geophys Union 75: 353

Brückner VR (1961) Zur Kinetik des Stoffaustausches an den Grenzflächen zwischen Silikatglas – und Salzschmelzen und des Stofftransportes in Silikatglasschmeltzen unter besonder-

er Berücksichtigung des Verhaltens von Na_2SO_4 und seinen Zersetzungsprodukten, Teil II. Glastech Ber 34: 515–528

Brückner VR (1962) Zur Kinetik des Stoffaustausches an den Grenzflächen zwischen Silikatglas – und Salzschmelzen und des Stofftransportes in Silikatglasschmelzen unter besonderer Berücksichtigung des Verhaltens von Na_2SO_4 und seinen Zersetzungsprodukten, Teil III. Glastech Ber 35: 93–105

Carroll M (1991) Diffusion of Ar in rhyolite, orthoclase and albite composition glasses. Earth Planet Sci Lett 103: 156–168

Carroll M, Rutherford MJ (1985) Sulfide and sulfate saturation in hydrous silicate melts. Proc 15th Lunar Planet Sci Conf, J Geophys Res 90: C601–C612

Carroll M, Rutherford MJ (1987) The stability of igneous anhydrite: experimental results and implications for sulfur behavior in the 1982 El Chichon trachyandesite and other evolved magmas. J Petrol 28: 781–801

Carroll M, Rutherford MJ (1988) Sulfur speciation in hydrous experimental glasses of varying oxidation state: results from measured wavelength shifts of sulfur x-rays. Am Mineral 73: 845–849

Crank J (1975) The mathematics of diffusion (2nd edn). Oxford University Press, Oxford

Devine JD, Sigurdsson H, Davis AN, Self S (1984) Estimates of sulfur and chlorine yield to the atmosphere from volcanic eruptions and potential climate effects. J Geophys Res 89: 6309–6325

Devine JD, Gardner JE, Brach HP, Layne GD, Rutherford MJ (1994) Comparison of microanalytical methods for estimation of H_2O contents of silicic volcanic glasses. Am Mineral, in press

Gerlach TM, McGee KA (1994) Total sulfur dioxide emissions and pre-eruption vapor-saturated magma at Mount St. Helens 1980–1988. Geophys Res Lett 21: 2833–2836

Haughton DR, Roeder PL, Skinner BJ (1974) Solubility of sulfur in mafic magmas. Econ Geol 69: 451–467

Jambon A (1982) Tracer diffusion in granitic melts: experimental results for Na, K, Rb, Cs, Ca, Sr, Ba, Ce, Eu to 1300° C and a model of calculation. J Geophys Res 87: 10,797–10,810

Katsura T, Nagashima S (1974) Solubility of sulfur in some magmas at 1 atm pressure. Geochim Cosmochim Acta 38: 517–531

Luhr JF (1990) Experimental phase relations of water- and sulfur-saturated arc magmas and the 1982 eruptions of El Chichón volcano. J Petrol 31: 1071–1114

Luhr JF, Carmichael ISE, Varekamp JC (1984) The 1982 eruptions of El Chichón volcano, Chiapas, Mexico: mineralogy and petrology of the anhydrite-bearing pumices. J Volcanol Geotherm Res 23: 69–108

Mathez EA (1976) Sulfur solubility and magmatic sulfides in submarine basalt glass. J Geophys Res 81: 4269–4276

Nagashima S, Katsura T (1973) The solubility of sulfur in Na_2O-SiO_2 melts under various oxygen partial pressures at 1100, 1250 and 1300° C. Bull Chem Soc Jap 46: 3099–3103

Nielsen CH, Sigurdsson H (1981) Quantitative methods of electron microprobe analysis of sodium in natural and synthetic glasses. Am Mineral 66: 547–552

Nilsson K, Peach CL (1996) Sulfur speciation, oxidation state, and sulfur concentration in backarc magmas. Geochim Cosmochim Acta 57: 3807–3813

Rutherford MJ, Devine JD (1996) Pre-eruption pressure-temperature conditions and volatiles in the 1991 dacitic magma of Mount Pinatubo. US Geol Surv Spec Pap, in press

Rutherford MJ, Hill P (1993) Magma ascent rates from amphibole breakdown: and experimental study applied to the 1980–1986 Mount St. Helens eruptions. J Geophys Res 98: 19,667–19,685

Schreiber HD, Kozak SJ, Fritchman AL, Goldman DS, Schaeffer HA (1986) Redox kinetics and oxygen diffusion in a borosilicate melt. Phys Chem Glasses 27: 152–177

Shannon RD (1976) Revised effective atomic radii and systematic studies of interatomic distances in halides and chalcogenides. Acta Crystallogr A25: 925–946

Stolper E (1982) Water in silicate glasses: an infrared spectroscopic study. Contrib Mineral Petrol 81: 1–17

Wallace PJ, Carmichael ISE (1992) Sulfur in basaltic magmas. Geochim Cosmochim Acta 56: 1863–1874

Watson EB (1991) Diffusion of dissolved CO_2 and Cl in hydrous silicic to intermediate magmas. Geochim Cosmochim Acta 55: 1897–1902

Watson EB (1994) Diffusion in volatile-bearing magmas. In: Carroll MR, Holloway JR (eds) Volatiles in magmas (Reviews in Mineralogy vol. 30). Mineralogical Society of America, Washington DC, pp 371–409

Watson EB, Wark DA, Delano JW (1993) Initial report on sulfur diffusion in magmas. EOS Trans Am Geophys Union 74: 620

Wendlandt RF (1991) Oxygen diffusion in basalt and andesite melts: experimental results and discussion of chemical versus tracer diffusion. Contrib Mineral Petrol 108: 463–471

Westrich HR, Gerlach TM (1992) Magmatic gas source for the stratospheric SO_2 cloud from the June 15 1991 eruption of Mount Pinatubo. Geology 20: 867–870

Zhang Y, Stolper EM, Wasserburg GJ (1991) Diffusion of water in rhyolitic glasses. Geochim Cosmochim Acta 55: 441–456